Second-Order Nonlinear Optical Effects of Spin Currents

Jing Wang,[1,2] Bang-Fen Zhu,[2,3] and Ren-Bao Liu[1,*]

[1]*Department of Physics, The Chinese University of Hong Kong, Shatin, N.T., Hong Kong, China*
[2]*Department of Physics, Tsinghua University, Beijing 100084, China*
[3]*Institute of Advanced Study, Tsinghua University, Beijing 100084, China*

Pure spin currents carry information in spintronics and signify novel quantum spin phenomena such as topological insulators. Measuring pure spin currents, however, is difficult since they have no direct electromagnetic induction. Noticing that a longitudinal spin current, in which electrons move along their spin directions, is a chiral quantity, we envisage that it has a chiral sum-frequency optical effect. A systematic symmetry analysis confirms this idea and reveals the second-order optical effects of general spin currents with unique polarization dependence. Microscopic calculations based on the eight-band model of III-V compound semiconductors show that the susceptibility is sizable under realistic conditions. These findings form a basis for ''seeing'' spin currents where and while they flow with standard nonlinear optical spectroscopy, providing a toolbox to explore a wealth of physics connecting spins and photons.

Pure spin currents (PSCs), which are made of opposite spins moving with opposite velocities, carry information via spins in lieu of charges and play a key role in spintronics [1,2]. They also signify the occurrence of some novel spin-related quantum phenomena such as the spin Hall effect [3–10] and topological insulators [11–15]. Spin currents were previously observed via spin accumulation at stopping edges [7–9,16] or conversion to electrical signals [10,17–19]. Direct and nondestructive measurement of PSCs where and while they flow [20,21] is highly desired, but is very difficult because a PSC bears neither net charge current nor net magnetization and therefore has no direct electromagnetic induction. A previous scheme of detecting a PSC by a ''photon spin current'' carried by a polarized light beam [20] is limited by weak interaction since the photon current involves the tiny light momentum. Recently, a remarkable experiment [21] showed coupling between a spin current and a spin wave. As a direct probe of spin currents, however, the spin-wave technique requires special design and fabrication of magnetic nanostructures.

In this Letter, we present a conceptually new aspect, namely, second-order nonlinear optical effects, of spin currents resulting from their unique physical nature and symmetry properties. Noticing that a longitudinal spin current, in which the spins point parallel or antiparallel to the current, is a chiral quantity, we envisaged that it can be probed by the chiral sum-frequency optical spectroscopy which was recently developed to detect molecular chirality [22–24]. By symmetry analysis in general cases and microscopic calculations in realistic models, we discovered that a PSC has sizable second-order optical susceptibility. This finding lays the foundation of direct, nondestructive measurement of spin currents by standard optical spectroscopy, facilitating application of spintronics [1,2] and research on spin-related physics [3–15].

Spin currents have peculiar symmetry properties owing to the characteristics of spins. A spin is an axial vector. As illustrated in Fig. 1(a), a spin reverses inside a parallel mirror and is unchanged inside a perpendicular mirror, the opposite of a usual vector. When particles move parallel or antiparallel to their spin directions, a longitudinal spin current results, which has a special symmetry property— chirality, as illustrated in Fig. 1(b): If a spin's microscopic current circulates its moving direction left-handedly, the mirror image does right-handedly, and vice versa.

The chiral sum-frequency effect of a longitudinal spin current is illustrated as follows. In chiral sum frequency, two input optical fields $\mathbf{F}_1$ and $\mathbf{F}_2$ (with frequencies ω_1 and ω_2, respectively) and the induced polarization field $\mathbf{P}$ at frequency $\omega_1 + \omega_2$ form a left- or right-hand system. Figure 1(c) shows how a chiral sum-frequency process occurs in a chiral system. Considering a right-hand helix, a charge at position A will be driven to point B by an electric field $\mathbf{F}_1$, which is along the X axis, and then to point C by $\mathbf{F}_2$, which is along the Y axis. The confinement of the helix leads to a net displacement along the Z axis. Thus $(\mathbf{F}_1, \mathbf{F}_2, \mathbf{P})$ form a right-hand system. If the order of input fields is reversed ($\mathbf{F}_2$ applies before $\mathbf{F}_1$), the charge would follow a trajectory like $D \to E \to F$, resulting in a polarization along the $-Z$ axis, and $(\mathbf{F}_2, \mathbf{F}_1, \mathbf{P})$ still form a right-hand system. Similarly, the sum frequency in a left-hand helix is a left-hand chiral process. A sum-frequency process is characterized by a second-order susceptibility $\chi^{(2)}$ via $\mathbf{P}(\omega_1 + \omega_2) = \chi^{(2)} : \mathbf{F}_1(\omega_1)\mathbf{F}_2(\omega_2)$. In the above example of helix, the susceptibility may be written as a form of three dyadic vectors, $\chi^{(2)} = A(\mathbf{ZYX} - \mathbf{ZXY})$, i.e., a rank-3 tensor. Thus the chiral sum-frequency susceptibility provides a measurement of the chirality of a physical object. If otherwise measured in linear optics, the effect of the chirality relies on the small magnetic moment of the molecules, and in turn on the small wave vector of
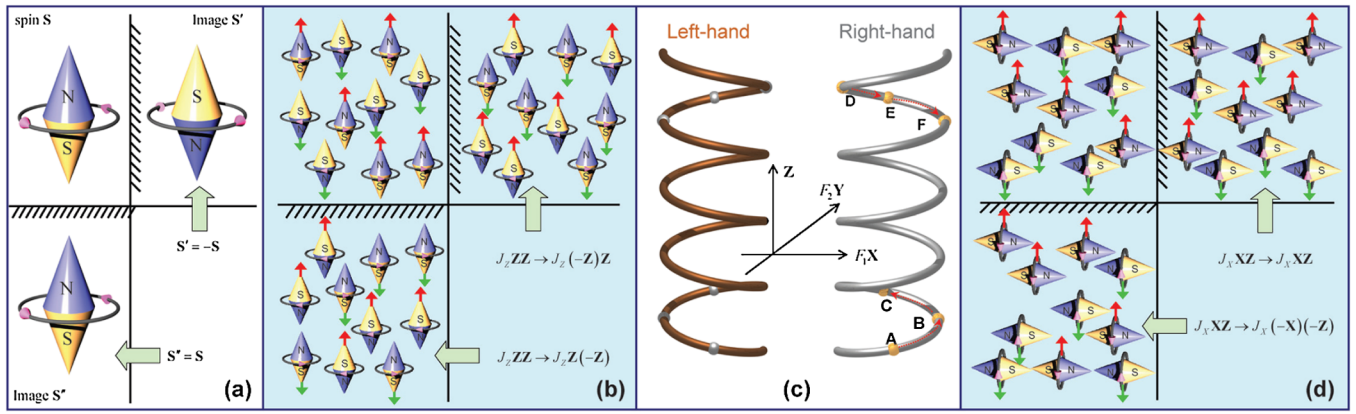
FIG. 1 (color online).   Symmetry analysis for sum-frequency effects of spin currents. (a) A spin under mirror reflections. (b) A longitudinal spin current under mirror reflections. The arrows indicate the moving directions of the spins. (c) Chiral sum-frequency processes in chiral systems. (d) A transverse spin current under mirror reflections.

the probe light, similar to the case of linear optical effects of spin currents [20].

For a systematic symmetry analysis, we consider a spin current with both longitudinal and transverse components. We define the Z axis as the current direction and the X axis as the spin direction of the transverse component. The spin current can be written as a rank-2 tensor $\mathbb{J} = J_X \mathbf{XZ} + J_Z \mathbf{ZZ}$, in a form of dyadic vectors, in which the left (right) vector is the spin (current) direction and $J_{Z(X)}$ is the longitudinal (transverse) amplitude. Above all, the spin current breaks the inversion symmetry, making possible a second-order optical process [25].

In general, the sum-frequency susceptibility tensor has 27 independent terms, $\chi^{(2)} = \chi_{XXX}\mathbf{XXX} + \chi_{XXY}\mathbf{XXY} + \cdots + \chi_{ZZZ}\mathbf{ZZZ}$, but the symmetry properties of a spin current will set many terms to be zero or nonindependent [25]. For a longitudinal spin current, only the chiral terms are nonzero. In a nonchiral term, at least

one of the three directions $\mathbf{X}$, $\mathbf{Y}$, and $\mathbf{Z}$ appears even times (twice or zero times). Consider $\chi_{XXY}\mathbf{XXY}$ for example. Under reflection by the Y-Z plane, the longitudinal spin current is reversed, but $\chi_{XXY}\mathbf{XXY}$ is unchanged, so this term must be zero. Similar arguments apply to other nonchiral terms. Also, the susceptibility must be antisymmetric under reflection by any plane parallel to the Z axis. With these constraints, the sum-frequency susceptibility of a longitudinal spin current can be written as

$$\chi^{(2)}_{J_Z} = J_Z[\alpha_1(\mathbf{XYZ} - \mathbf{YXZ}) + \alpha_2(\mathbf{YZX} - \mathbf{XZY}) + \alpha_3(\mathbf{ZXY} - \mathbf{ZYX})], \tag{1}$$

with only three independent parameters. As for a transverse spin current $J_X \mathbf{XZ}$, it changes its sign under reflection by the X-Z plane but is invariant under reflection by the X-Y or Y-Z plane [see Fig. 1(d)], each nonzero term in the susceptibility must contain odd times of $\mathbf{Y}$ and even
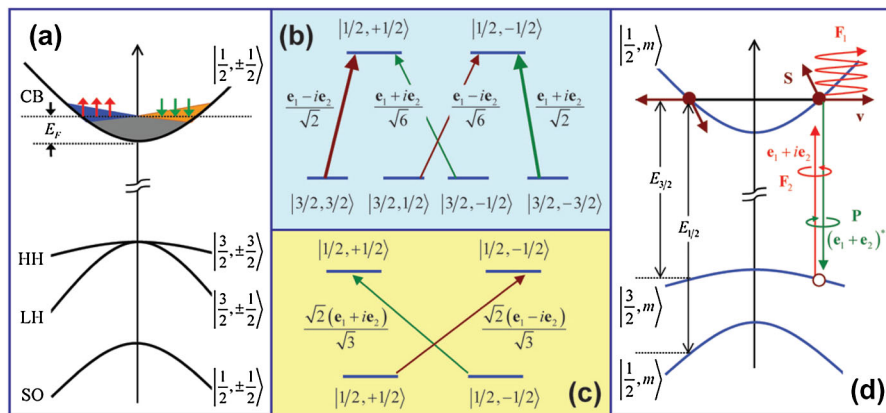

FIG. 2 (color online).   Models for microscopic calculation of the sum-frequency susceptibility. (a) The full eight-band model and the electron spin distribution for a PSC in a semiconductor. (b) and (c) Selection rules and relative dipole moments from the spin-3/2 and spin-1/2 valence bands to the conduction band, respectively. (d) A simplified model with the HH-LH splitting neglected, in which the spin states and selection rules for interband transitions can be defined independent of the momentum. The transition energies to the Fermi surface from different valence bands are indicated.
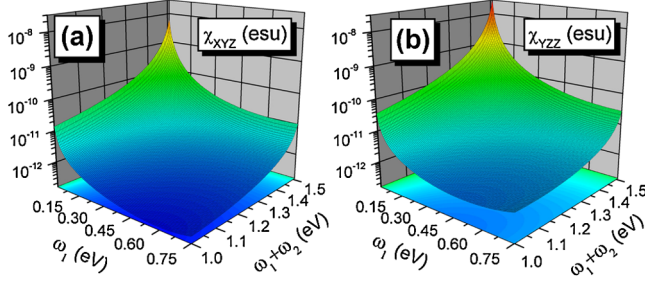
FIG. 3 (color online). Representative results of the sum-frequency susceptibility. (a) χ_{XYZ} due to a longitudinal spin current, and (b) χ_{YZZ} due to a transverse spin current, as functions of the optical frequencies. Parameters are chosen similar to those in Ref. [7]: The band gap is 1519 meV, the HH-SO splitting is 341 meV, the doping concentration is 3×10^{16} cm^{-3}, the effective mass (in units of free electron mass) of the HH, LH, SO, and conduction bands is in turn 0.45, 0.082, 0.15, and 0.067, the dipole $d_{cv} = 6.7$ eÅ, the dielectric constant $\varepsilon_r = 10.6$, and the spin current $J_X = J_Z = 20$ nA/μm^2.

times of **Z** or **X**, so

$$\chi_{J_X}^{(2)} = J_X(x_1 \mathbf{XXY} + x_2 \mathbf{XYX} + x_3 \mathbf{YXX} + z_1 \mathbf{ZZY}$$
$$+ z_2 \mathbf{ZYZ} + z_3 \mathbf{YZZ} + y \mathbf{YYY}), \qquad (2)$$

with seven independent parameters. The unique polarization dependence of the second-order susceptibility of a spin current can be used to distinguish its transverse and longitudinal components, and also to single out the spin-current signature from the effects of the material background or a charge current [26].

To determine the independent parameters of the susceptibility in Eqs. (1) and (2), we performed microscopic calculation for a PSC in a bulk GaAs, using the standard perturbation theory [25,27] with an eight-band model [28]. We assumed that the pure spin-current result from a non-equilibrium distribution of electrons in the conduction band, with a small portion of electrons near the Fermi surface having opposite spin polarizations for opposite velocities [Fig. 2(a)], under conditions similar to those in Ref. [7]. The optical interaction includes the interband transitions and the intraband acceleration of electrons and holes. To avoid real absorption of light, the light frequencies were chosen such that the sum frequency is below the band gap. For the sake of simplicity, we neglected the anisotropy of the valence bands. We also neglected the Coulomb interaction, since it is largely screened in the n-doped material. These approximations, according to the symmetry analysis, would only quantitatively modify the results. The spin splitting due to the bulk inversion asymmetry of the material (the Dresselhaus effect) is as small as 0.01 meV for the doping level considered (3×10^{16} cm^{-3}), and therefore was neglected. The bulk inversion asymmetry would cause a background second-order susceptibility, which is indeed strong but can be well separated from the spin-current effect by ac modulation

of the current and phase-locking detection. Two representative results of the calculated susceptibility spectra are shown in Fig. 3. The other terms of the susceptibility tensor (not shown) have similar frequency dependence and comparable amplitudes. As a specific example, a transverse spin current 20 nA/μm^{-2} has a susceptibility $\chi_{YZZ} \approx 0.40 \times 10^{-9}$ esu (or 0.17×10^{-12} m/V in SI units) for input frequencies $\omega_1 = 100$ meV and $\omega_2 = 1,400$ meV, or $17. \times 10^{-12}$ esu for $\omega_1 = \omega_2 = 750$ meV (corresponding to the second harmonics generation).

To better understand the microscopic mechanism of the sum-frequency effect of a spin current, we simplify the model by neglecting the splitting between the heavy hole (HH) band and the light hole (LH) band. Under this approximation, the HH and LH bands form a spin-3/2 band with fourfold degeneracy. The split-off (SO) band and the conduction band have spin-1/2. Thus the spin states and the selection rules for interband transitions are separated from the momentum [Figs. 2(b) and 2(c)].

Let us consider a single electron with momentum **k** and spin polarization $\mathbf{s_k}$ [Fig. 2(d)]. We set up a coordinate system $(\mathbf{e}_1, \mathbf{e}_2, \mathbf{e}_3)$ so that $\mathbf{s_k} = \mathbf{e}_3(f_+ - f_-)/2$ with $f_{+/-}$ denoting the population at the spin-up or -down state. The angular momentum conservation requires that a light with circular polarization $\mathbf{e}_1 \pm i\mathbf{e}_2$ couples only to the transitions $|j, m\rangle \leftrightarrow |1/2, m \pm 1\rangle$, where $j = 3/2$ or $1/2$ is the spin of a valence band and $m = -j, j + 1, \ldots$, or j is the component along the $\mathbf{e}_3$ axis. The relative dipole moments of the relevant interband transitions are indicated in Figs. 2(b) and 2(c). To simplify the discussion, we set the input frequency ω_2 to be near resonant with the band gap and much greater than ω_1, so that the interband transitions and the intraband driving are mostly caused by $\mathbf{F}_2 \exp(-i\omega_2 t_2)$ and $\mathbf{F}_1 \exp(-i\omega_1 t_1)$, respectively.

We first examine interband transitions. For example, the transition $|3/2, -3/2\rangle \rightarrow |1/2, -1/2\rangle$ generated from the time t_2 to $t_2 + dt_2$ has a probability amplitude $dG_2 = i(1 - f_-)(d_{cv}^*/\sqrt{2})(\mathbf{e}_1 + i\mathbf{e}_2)^* \cdot \mathbf{F}_2 \exp(-i\omega_2 t_2)dt_2$, where d_{cv} is the interband dipole, and the factor $(1 - f_-)$ accounts for the Pauli blocking. After the excitation, the probability amplitude oscillates with frequency $E_{3/2}(\mathbf{k})$, leading to the optical polarization $(\mathbf{e}_1 + i\mathbf{e}_2) \times (d_{cv}/\sqrt{2})e^{-iE_{3/2}(\mathbf{k})(t-t_2)}dG_2$ at time t, where $E_{3/2}(\mathbf{k}) = k^2/(2m_e) + k^2/(2m_{3/2})$ is the transition energy of a pair of electron and hole with mass m_e and $m_{3/2}$, respectively. The radiation has the same circular polarization as the input because of the angular momentum conservation. Summation over all possible transitions and integration over time give the linear optical response to the field $\mathbf{F}_2$ as

$$\mathbf{P}^{(1)}(t) = \frac{i}{3}|d_{cv}|^2 \int_{-\infty}^{t} e^{-i\int_{t_2}^{t} E_{3/2}(\mathbf{k})d\tau} \sum_{\pm}(1 - f_\pm)$$
$$\times (\mathbf{e}_1 \mp i\mathbf{e}_2)(\mathbf{e}_1 \mp i\mathbf{e}_2)^* \cdot \mathbf{F}_2 e^{-i\omega_2 t_2}dt_2. \qquad (3)$$

Thus $\mathbf{P}^{(1)} \propto s_k(\mathbf{e}_1\mathbf{e}_2 - \mathbf{e}_2\mathbf{e}_1) \cdot \mathbf{F}_2 = \mathbf{F}_2 \times \mathbf{s_k}$, which has a

transparent physical meaning: The linear polarization of the output field is related to that of the input one by a rotation about the spin, essentially a Faraday rotation due to the spin acting as a magnet. When the effect of the intraband driving by $\mathbf{F}_1$ is included, the momentum $\mathbf{k}$ should be replaced with the accelerated one $\tilde{\mathbf{k}}_\tau \equiv \mathbf{k} - e\mathbf{F}_1 \int_{-\infty}^{\tau} \exp(-i\omega_1 t_1)dt_1$ at time τ. By expansion to the linear order of $\mathbf{F}_1$, we have $\tilde{k}_\tau^2 \approx k^2 - 2e\mathbf{k} \cdot \mathbf{F}_1 \int_{-\infty}^{\tau} \exp(-i\omega_1 t_1)dt_1$, so the second-order optical response can be written as $\mathbf{P} \propto \mathbf{F}_2 \times \mathbf{s_k}e\mathbf{v_k} \cdot \mathbf{F}_1$, where $\mathbf{v_k} \equiv \mathbf{k}/m_e$ is the velocity of the electron with momentum $\mathbf{k}$. The physical meaning of $e\mathbf{v_k} \cdot \mathbf{F}_1$ is the power done by the field to the electron. $e\mathbf{s_k v_k}$ is just the spin-current tensor contributed by the electron.

For a distribution of electrons, the summation over the momentum space gives the sum-frequency response as $\mathbf{P} = \zeta\mathbf{F}_2 \times (\mathbb{J} \cdot \mathbf{F}_1)$, with

$$\zeta = \left(\frac{\varepsilon_r + 2}{3}\right)^3 \frac{(2/3)|d_{\text{cv}}|^2(1 + m_e/m_{3/2})}{(\omega_1 + \omega_2 - E_{3/2})(\omega_2 - E_{3/2})\omega_1}$$
$$- (E_{3/2}, m_{3/2} \rightarrow E_{1/2}, m_{1/2}), \quad (4)$$

derived by Fourier transformation of Eq. (3) including the intraband driving and the contribution of the SO band, where the factor containing the material dielectric constant ε_r takes into account the difference between the macroscopic external field and the microscopic local field [29], m_j denotes the mass of the spin-j hole band, and E_j is the transition energy from the spin-j band to the Fermi surface [see Fig. 2(d)]. The constants in Eqs. (1) and (2) are such that $\alpha_1 = -z_2 = z_3 = \zeta$ and others $= 0$. With the HH-LH splitting neglected, the sum-frequency susceptibility has a compact form with only one independent parameter. This feature is due to the separation of the spin and motion degrees of freedom of the electrons and holes. When the HH-LH splitting is nonzero, the spin quantization direction and therefore the optical selection rules depend on the momentum and vary with acceleration of the particles (a Berry curvature effect). This leads to the general form of susceptibility in Eqs. (1) and (2), with the extra terms proportional to the HH-LH splitting.

In summary, with systematic symmetry analysis in general cases and microscopic calculation under realistic conditions, we have shown that a pure spin current has a sizable sum-frequency susceptibility. In particular, a longitudinal spin current has a chiral sum-frequency effect. The current results can be straightforwardly extended to other second-order optical spectroscopy such as difference-frequency and three-wave mixing [25]. With universality of the method guaranteed by the symmetry principle and without requirements of resonance conditions or special structure design and fabrication, the nonlinear optical spectroscopy can be applied to study a wide range of spin-related quantum phenomena such as topological insulators [11–15]. A wealth of physics connecting spins and photons and technologies synthesizing spintronics and photonics may be explored.

*To whom correspondence should be addressed.
rbliu@phy.cuhk.edu.hk

[1] S. A. Wolf *et al.*, Science **294**, 1488 (2001).
[2] I. Zutic, J. Fabian, and S. Das Sarma, Rev. Mod. Phys. **76**, 323 (2004).
[3] M. I. Dyakonov and V. I. Perel, Phys. Lett. A **35**, 459 (1971).
[4] J. E. Hirsch, Phys. Rev. Lett. **83**, 1834 (1999).
[5] S. Murakami, N. Nagaosa, and S. C. Zhang, Science **301**, 1348 (2003).
[6] J. Sinova *et al.*, Phys. Rev. Lett. **92**, 126603 (2004).
[7] Y. K. Kato *et al.*, Science **306**, 1910 (2004).
[8] J. Wunderlich *et al.*, Phys. Rev. Lett. **94**, 047204 (2005).
[9] H. Zhao *et al.*, Phys. Rev. Lett. **96**, 246601 (2006).
[10] S. O. Valenzuela and M. Tinkham, Nature (London) **442**, 176 (2006).
[11] C. L. Kane and E. J. Mele, Phys. Rev. Lett. **95**, 226801 (2005).
[12] B. A. Bernevig, T. L. Hughes, and S. C. Zhang, Science **314**, 1757 (2006).
[13] M. König *et al.*, Science **318**, 766 (2007).
[14] D. Hsieh *et al.*, Nature (London) **460**, 1101 (2009).
[15] P. Roushan *et al.*, Nature (London) **460**, 1106 (2009).
[16] M. J. Stevens *et al.*, Phys. Rev. Lett. **90**, 136603 (2003).
[17] I. Appelbaum, B. Q. Huang, and D. J. Monsma, Nature (London) **447**, 295 (2007).
[18] S. D. Ganichev *et al.*, Phys. Rev. B **75**, 155317 (2007).
[19] X. D. Cui *et al.*, Appl. Phys. Lett. **90**, 242115 (2007).
[20] J. Wang, B. F. Zhu, and R. B. Liu, Phys. Rev. Lett. **100**, 086603 (2008); see also **101**, 069902(E) (2008).
[21] V. Vlaminck and M. Bailleul, Science **322**, 410 (2008).
[22] M. A. Belkin *et al.*, Phys. Rev. Lett. **85**, 4474 (2000).
[23] J. Wang *et al.*, Proc. Natl. Acad. Sci. U.S.A. **102**, 4978 (2005).
[24] N. Ji *et al.*, J. Am. Chem. Soc. **128**, 8845 (2006).
[25] Y. R. Shen, *The Principles of Nonlinear Optics* (Wiley-Interscience, New York, 1984).
[26] J. B. Khurgin, Appl. Phys. Lett. **67**, 1113 (1995).
[27] J. E. Sipe and A. I. Shkrebtii, Phys. Rev. B **61**, 5337 (2000).
[28] P. Y. Yu and M. Cardona, *Fundamentals of Semiconductors: Physics and Material Properties*, (Springer-Verlag, Berlin, 2005), 3rd ed.
[29] N. Bloembergen, *Nonlinear Optics* (Benjamin, New York, 1965).